thienyl)pyrazol-1-yl)]$_3^-$ may thus be of value in fine-tuning systems where HB(pz)$_3^-$ and HB(3,5-Me$_2$pz)$_3^-$ have been used until now. That the effect is steric, and unrelated to the pK_a of the respective pyrazoles, can be deduced from the reactivity of the 3-H-, 3-Me-, and 3-Ph-substituted tris(pyrazolyl)borates, which is H > Me > Ph, while their pK_a values are 2.48, 3.27, and 2.09, respectively.[25] The pK_a value for 3-thienylpyrazole is unknown.

(24) One of the reviewers suggested determining the cone angles for L*. We have determined the cone angle of the excluded space around Co during rotation of L* around the B–Co axis, with the thienyl group positioned so that its 3-H was in the closest proximity to Co. The "cone angle" thus obtained was 246°, while the "cone angle" for HB(3-Ph-pz)$_3$, determined in the same fashion, was 235°. Noting that the cone angle for the extremely hindered HB(3-Bu^{t}pz)$_3$ is 244°, one sees there is clearly no correlation between the calculated cone angles and the accessibility of the metal to nucleophilic reagents. Thus, the "cone angles" calculated for tris(pyrazolyl)borate ligands with planar 3-substituents are not meaningful. What is meaningful is the size of the open wedgelike spaces between the pz rings, as defined by the size and orientation of the 3-substituents, through which a nucleophile ligand can approach the metal center. Due to the variety of equilibrium geometries for the planar 3-substituents, calculation of these "wedge angles" is difficult. For 3-substituents such as H, Me, and Bu^t these wedge angles are 120, 91, and 67°, respectively, reflecting in a qualitative way the ease of access to the metal.

Acknowledgment. We wish to acknowledge W. Marshall for expert assistance with the X-ray data collection and crystal growth work and N. Jones for assistance in the preparation of the crystallographic tables and drawings. G.J.L. thanks Dr. F. Grandjean for many helpful discussions and also the donors of the Petroleum Research Fund, administered by the American Chemical Society, for support of this work.

Supplementary Material Available: Full summaries of X-ray diffraction data (Tables I-S and II-S) and listings of thermal parameters (Tables X and XI), hydrogen atom positions (Tables XII and XIII), and complete bond distances and angles (Tables XIV and XV) (13 pages); listings of observed and calculated structure factors (Tables XVI and XVII) (22 pages). Ordering information is given on any current masthead page.

(25) Catalan, J.; Abboud, J. L. M.; Elguero, J. *Adv. Heterocycl. Chem.* **1987**, *41*, 187–274.

Contribution from the Laboratory of Applied Quantum Chemistry, Faculty of Chemistry, University of Thessaloniki, P.O.B. 135, 54006 Thessaloniki, Greece, Institut fur Anorganische und Analytische Chemie, Freie Universitat, Berlin Fabeckstrasse 34-36, 1000 Berlin 33, West Germany, and Institute of Chemistry, University of Wroclaw, 14 F. Joliot-Curie Street, 50383 Wroclaw, Poland

Strong Ferromagnetism between Copper(II) Ions Separated by 6.7 Å in a New Phthalato-Bridged Copper(II) Binuclear Complex

Saleh K. Shakhatreh,[1a] Evangelos G. Bakalbassis,[1a] Irene Brüdgam,[1b] Hans Hartl,[1b] Jerzy Mrozinski,[1c] and Constantinos A. Tsipis*,[1a]

Received October 12, 1989

The crystal structure of [(dien)(ClO$_4$)Cu(1)(μ-Phth)Cu(2)(dien)](ClO$_4$), where Phth^{2-} is the dianion of phthalic acid and dien is diethylenetriamine, has been determined by direct X-ray methods. The complex crystallizes in the monoclinic space group $P2_1$ with two formula units in a unit cell of dimensions a = 12.101 (6) Å, b = 7.805 (4) Å, c = 15.415 (7) Å, β = 109.82 (4)°, and ρ_{calcd} = 1.690 g/cm^3. The structure was refined to conventional discrepancy factors of R = 0.054 and R_w = 0.060 for 2173 observed reflections. The acentric monoclinic cell contains binuclear cations [(dien)(ClO$_4$)Cu(1)(μ-Phth)Cu(2)(dien)]$^+$ and isolated perchlorate anions. The Cu centers are bridged by Phth dianions coordinated in both uni- and bidentate fashions to Cu(1) and Cu(2), respectively, through their carboxylic oxygen donor atoms. The two copper environments are dissimilar and irregular. The structure around Cu(1) is close to a square-based pyramid with one of the oxygen atoms of the perchlorate anions in the apical position. The Cu(2) environment is close to a severely distorted octahedron. An oxygen atom of a carboxylato group bridges two Cu(2) atoms of two different binuclear units, rather loosely [Cu(2)–O(22) = 2.318 (8) Å], to infinite chains of binuclear units around a screw axis 2_1. Least-squares fitting of the variable-temperature (4.2–295 K) magnetic susceptibility experimental data to Bleaney–Bowers equation with a molecular field approximation led to a singlet–triplet energy gap of 80 ± 10 cm^{-1}, g = 2.10, and zJ' = −1.81 cm^{-1}. The EPR spectrum does not exhibit any evidence of triplet state. From an orbital interpretation of the coupling stems a new situation leading to ferromagnetic interaction between magnetic centers separated by multiatom-bridging units.

Introduction

Copper(II) binuclear complexes exhibiting a spin–triplet ground state are very few[2] as compared to those with a spin–singlet ground state. To our knowledge, in all three known cases of ferromagnetically coupled molecular magnetic systems the two magnetic centers are bridged by a single-atom bridging ligand. The ferromagnetic properties of these compounds have been attributed[2,3] either to the accidental or to strict orthogonality of their magnetic orbitals and/or to spin-polarization effects. With this in mind we thought it would be advisable to explore further the fascinating field of molecular ferromagnets. As a consequence, we focused our efforts on the investigation of novel ferromagnetically coupled Cu(II) magnetic systems involving magnetic centers far separated from each other via multiatom–bridging units. Phthalate dianions, due to both their versatile bonding mode with the Cu(II) ions[4] and their peculiar structure—involving carboxylate groups that are noncoplanar with themselves and with the benzene ring—could be good candidates in supporting long-distance ferromagnetic exchange interactions. Within this framework and following our continuing experience on the magnetostructural correlations in multiatom-bridged exchange-coupled systems,[5-7] we came across

(1) (a) University of Thessaloniki. (b) Berlin's Freie Universität. (c) Univeristy of Wroclaw.
(2) Kahn, O. *Comments Inorg. Chem.* **1984**, *3*, 105.
(3) Willett, R. D.; Gatteschi, D.; Kahn, O., Eds. *Magnetostructural Correlations in Exchange Coupled Systems* (Nato Advanced Study Institute Series); D. Reidel: Dordrecht, The Netherlands, 1984.
(4) (a) Biagini, M. C.; Manotti Lanfredi, A. M.; Tiripicchio, A.; Tiripicchio, C. M. *Acta Crystallogr.* **1981**, *B37*, 2159. (b) Krstanovic, I.; Karanovic, Lj.; Stojakovic, Dj.; Golic, Lj. *Cryst. Struct. Commun.* **1982**, *11*, 1747. (c) Prout, C. K.; Carruthers, J. R.; Rossotti, F. F. C. *J. Chem. Soc. A* **1971**, 3350.

0020-1669/91/1330-2801$02.50/0

Table I. Crystallographic Data for $[Cu_2(dien)_2(\mu\text{-Phth})](ClO_4)_2$

chem formula	$C_{16}H_{30}Cl_2Cu_2N_6O_{12}$	V, Å^3	1369.68
fw	696.49	Z	2
space group	$P2_1$ (No. 4)	λ(Cu Kα), Å	1.5418
T, °C	20	ρ_{obsd}, g cm^{-3}	1.688
a, Å	12.101 (6)	ρ_{calcd}, g cm^{-3}	1.690
b, Å	7.805 (4)	μ, cm^{-1}	43.60
c, Å	15.415 (7)	$R(F_o)$	0.054
β, deg	109.82 (4)	$R_w(F_o)$	0.060

with the first phthalato-bridged dimeric Cu(II) complex[8] exhibiting a spin–triplet ground state.

In this work we report the synthesis, crystal structure, and magnetic properties of the first multiatom-bridged ferromagnetically coupled Cu(II) complex, formulated as $[(dien)(ClO_4)Cu(1)(\mu\text{-Phth})Cu(2)(dien)](ClO_4)$. To our knowledge, this is the first example of a large ferromagnetic interaction between Cu(II) ions separated by 6.7 Å. Finally, a possible interpretation of its magnetic behavior, based upon the structural and EHMO LCAO–MO quantum-chemical data, was attempted too.

Experimental and Computational Section

Synthesis. The complex was prepared by adding a methanolic solution (25 mL) of 0.89 mmol of the phthalate piperidinium salt to a methanolic solution (25 mL) of 1.78 mmol of $Cu(ClO_4)_2$ and 1.78 mmol of dien. The resulted dark blue microcrystalline solid gave, upon recrystallization from hot methanol, single crystals suitable for the structure and magnetic determinations. Anal. Calcd for $C_{16}H_{30}N_6O_{12}Cl_2Cu_2$: C, 27.59; H, 4.34; N, 12.07; O, 27.57; Cl, 10.18; Cu, 18.25. Found: C, 27.42; H, 4.29; N, 12.19; O, 27.69; Cl, 10.09; Cu, 18.32.

Physical Measurements. Infrared, reflectance, and EPR instrumentation, computational details, and the procedure for variable-temperature magnetic susceptibility determination have been previously described.[5]

Crystal Structure Determination and Refinement. Data collection was carried out on a STOE automated diffractometer (Cu Kα radiation, Ni filter, $\theta/2\theta$ scan). Unit cell parameters were based on least-squares refinement of the setting angles of 20 reflections ($80° < 2\theta < 120°$). The intensities of two standard reflections were measured every 90 min to monitor crystal decay and alignment. There was no crystal decay. A fragment of a crystal needle of approximate size 0.05 × 0.15 × 0.5 mm was used for intensity data collection. A total of 2215 unique reflections were measured at 293 K ($5° \le 2\theta \le 120°$) in the hemisphere $-13 \le h \le 12$, $0 \le k \le 8$, and $0 \le l \le 17$. A total of 2173 reflections were considered as observed ($I \ge 2\sigma(I)$). Data were corrected for Lorentz and polarization effects but not for absorption ($\mu_{Cu\,K\alpha} = 43.6$ cm^{-1}).

The structure was solved by direct methods and successive difference fourier syntheses, where most of the H atoms could be located; the missing ones were calculated. All atoms—with the exception of the H ones—were refined with anisotropic temperature factors. Scattering factors and dispersion coefficients used for the neutral atoms were taken from the *International Tables for X-ray Crystallography*, Vol. III. In the final cycles of least-squares refinement (the minimizing function being $\sum_i w_i(|F_o| - |F_c|)^2$) weights were calculated with $w = xy$ ($x = 1$ for $\sin\theta > 0.33$; $x = (\sin\theta)/0.33$ for $\sin\theta \le 0.33$; $y = 1$ for $F_o < 34.0$; $y = 34.0/F_o$ for $F_o \ge 34.0$). Several cycles of full-matrix least-squares refinement for 443 parameters and 2215 reflections, by use of this weighting scheme, converged to $R = 0.054$ and $R_w = 0.060$. Attempts to refine the alternative enantiomorphic structure or to consider an extinction correction did not result in a better agreement with the diffraction data. The maximum parameter shifts in the last cycle were less than 0.40 for all atoms, the exception being the H and the two O(6) and O(8) atoms of the perchlorate group. A final difference fourier map showed a maximum electron density of 0.9 e Å^{-3}. The crystallographic calculations were performed by using[9-11] the programs X-RAY 76, MITHRIL, and PLUTO.

General crystallographic information is given in Table I. A full-length table of crystallographic data is given as supplementary material (Table SI). The atomic parameters for the non-hydrogen atoms are shown in Table II. Main bond distances and bond angles are in Tables III and IV, respectively. Anisotropic thermal parameters, positional parameters for hydrogen atoms, and full-length tables for the bond dis-

Table II. Atomic Parameters and Esd's of the Non-Hydrogen Atoms

atom	x/a	y/b	z/c	$100U_{eq}$,[a] Å^2
Cu(1)	0.82237 (10)	0.24995 (36)	0.56510 (8)	5.03
Cu(2)	0.95567 (9)	0.24151 (32)	1.02409 (8)	4.09
Cl(1)	0.3839 (3)	0.0976 (5)	0.2265 (2)	5.8
Cl(2)	0.7884 (2)	−0.2088 (4)	0.5316 (2)	5.1
C(1)	1.0116 (8)	0.2032 (12)	0.7365 (6)	3.5
C(2)	1.1181 (7)	0.1690 (14)	0.9423 (6)	3.4
C(11)	0.6010 (8)	0.2005 (16)	0.5895 (9)	5.8
C(12)	0.5765 (9)	0.2910 (19)	0.5007 (8)	5.9
C(13)	0.7961 (12)	0.3056 (19)	0.3755 (8)	6.7
C(14)	0.6779 (11)	0.3484 (18)	0.3845 (8)	5.7
C(21)	0.8647 (10)	0.1879 (15)	1.1670 (7)	5.4
C(22)	0.9972 (10)	0.1766 (16)	1.2141 (7)	5.3
C(23)	0.7218 (8)	0.1645 (15)	1.0066 (7)	4.6
C(24)	0.7264 (9)	0.1288 (15)	0.9126 (8)	4.8
C(111)	1.1415 (7)	0.2187 (14)	0.7868 (6)	3.4
C(112)	1.2184 (7)	0.2599 (19)	0.7389 (6)	4.4
C(113)	1.3367 (8)	0.2753 (21)	0.7824 (7)	5.9
C(114)	1.3832 (7)	0.2490 (28)	0.8756 (7)	6.9
C(115)	1.3110 (8)	0.2083 (16)	0.9260 (6)	4.5
C(116)	1.1900 (8)	0.1950 (12)	0.8835 (6)	3.3
N(11)	0.8842 (8)	0.3192 (15)	0.4663 (6)	5.9
N(12)	0.6667 (7)	0.2436 (16)	0.4614 (5)	4.4
N(13)	0.7251 (7)	0.2312 (17)	0.6459 (6)	5.3
N(21)	1.0536 (6)	0.2666 (13)	1.1566 (5)	4.1
N(22)	0.8405 (7)	0.1327 (11)	1.0726 (6)	3.8
N(23)	0.8260 (6)	0.2266 (13)	0.9020 (5)	4.0
O(1)	0.2706 (8)	0.0371 (15)	0.2225 (7)	7.7
O(2)	0.4681 (8)	0.0496 (14)	0.3083 (6)	7.3
O(3)	0.4077 (12)	0.0287 (29)	0.1503 (8)	14.9
O(4)	0.3730 (13)	0.2851 (16)	0.2238 (14)	14.5
O(5)	0.8632 (10)	−0.3271 (19)	0.5192 (12)	13.3
O(6)	0.7612 (14)	−0.1708 (31)	0.6026 (11)	18.0
O(7)	0.6895 (8)	−0.1708 (16)	0.4537 (6)	7.8
O(8)	0.8614 (13)	−0.0601 (19)	0.5521 (18)	18.4
O(11)	0.9766 (5)	0.2713 (12)	0.6565 (4)	4.4
O(12)	0.9501 (5)	0.1267 (10)	0.7740 (5)	4.1
O(21)	1.0736 (5)	0.3030 (9)	0.9636 (4)	3.5
O(22)	1.1063 (6)	0.0218 (9)	0.9730 (5)	4.1

[a] $U_{eq} = {}^1/_3(U_{11} + U_{22} + U_{33})$.

Table III. Main Interatomic Distances (Å)[a]

		Cu–Cu	
intramolecular	6.704 (4)	shortest intrachain	4.180 (3)
		Cu Surroundings	
Cu(1)–O(11)	1.927 (5)	Cu(2)–O(21)	2.010 (7)
Cu(1)–N(11)	1.99 (2)	Cu(2)–N(21)	1.994 (7)
Cu(1)–N(12)	2.016 (7)	Cu(2)–N(22)	1.982 (9)
Cu(1)–N(13)	1.99 (1)	Cu(2)–N(23)	2.004 (6)
Cu(1)–O(8)	2.46 (2)	Cu(2)–O(22)	2.800 (8)
		Cu(2)–O(22′)[b]	2.318 (8)
		Bridging Phthalato Ligand	
C(1)–O(11)	1.28 (2)	C(2)–O(21),O(22)	1.27 (2)
C(1)–O(12)	1.24 (2)	C(2)–C(116)	1.47 (2)
C(1)–C(111)	1.50 (2)	C(111)–C(116)	1.42 (2)
C(111)–C(112)	1.41 (2)	C(112)–C(113)	1.36 (2)
		Diethylenetriamine Ligands	
N(11)–C(13)	1.45 (2)	N(21)–C(22)	1.47 (2)
C(13)–C(14)	1.52 (3)	C(22)–C(21)	1.52 (2)
C(14)–N(12)	1.48 (2)	C(21)–N(22)	1.45 (2)
N(12)–C(12)	1.46 (2)	N(22)–C(23)	1.47 (2)
C(11)–C(12)	1.48 (2)	C(23)–C(24)	1.49 (2)
		Perchlorate Anions	
Cl(1)–O(1)	1.43 (2)	Cl(2)–O(8)	1.43 (2)
Cl(1)–O(2)	1.377 (9)	Cl(2)–O(5)	1.35 (2)

[a] Standard deviations of the last significant figures are given in parentheses. [b] Symmetry operations: (′) $2 - x$, ${}^1/_2 + y$, $2 - z$; (″) $2 - x$, $-{}^1/_2 + y$, $2 - z$.

(5) (a) Bakalbassis, E. G.; Mrozinski, J.; Tsipis, C. A. *Inorg. Chem.* **1985**, *24*, 4231. (b) *Ibid.* **1986**, *25*, 3684.
(6) Bakalbassis, E. G.; Bozopoulos, A. P.; Mrozinski, J.; Rentzeperis, P. J.; Tsipis, C. A. *Inorg. Chem.* **1988**, *27*, 529.
(7) Shakhatreh, S. K. Ph.D. Thesis, University of Thessaloniki, Thessaloniki, Greece, 1987.
(8) Taken in part from ref 7.
(9) Stewart, J. M. Report TR-446, X-Ray 76; Computer Science Center, University of Maryland: College Park, MD, 1976.
(10) Gilmore, C. J. *J. Appl. Crystallogr.* **1984**, *17*, 42.
(11) PLUTO 78. Cambridge Crystallographic Data Base, Cambridge Crystallographic Data Center, 1979.

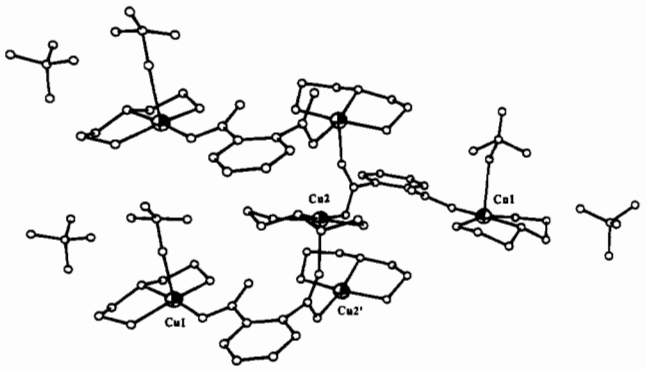

Figure 1. ORTEP perspective view of three symmetry-related units of the complex under study.

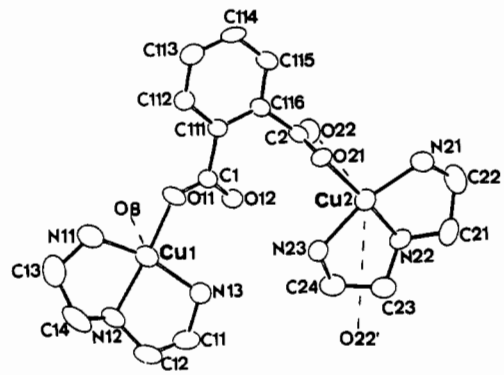

Figure 2. Molecular structure of the $[Cu_2(\mu\text{-Phth})(dien)_2(ClO_4)]^+$ binuclear unit.

tances and bond angles and observed and calculated factors (Tables SII–SVI) are available as supplementary material.

Results and Discussion

Description of the Structure. The acentric monoclinic unit cell contains polymeric cations $_\infty[(dien)(ClO_4)Cu(1)(\mu\text{-Phth})Cu(2)(dien)]^+$ and isolated perchlorate anions. An ORTEP[12] perspective view of three symmetry-related units is shown in Figure 1. The cations (Figure 2) consist of binuclear units with two Cu centers bridged by Phth dianions, coordinated in both uni- and bidentate fashions, to Cu(1) and Cu(2), respectively, through the oxygen atoms of their carboxylate groups. Moreover, O(22) bridges two Cu(2) centers of two different binuclear units, rather loosely [Cu(2)–O(22) = 2.800 (8) Å; Cu(2')–O(22) – 2.318 (8) Å]. Thus, infinite chains of polymeric cations around a screw axis 2_1 are derived. One of the two crystallographically independent perchlorate anions is coordinated, through one of its O atoms, to Cu(1); the other ClO_4^- anion is noncoordinated.

The two copper environments are dissimilar and irregular. The structure around Cu(1) could be described as a distorted square-based pyramid. The basal plane includes the three nitrogen atoms, N(11), N(12), and N(13), of a dien ligand as well as the O(11) atom of the first carboxylato group of the Phth anion. The apical position is occupied by the O(8) atom of the coordinated perchlorate group [Cu(1)–O(8) = 2.46 (2) Å]. The largest deviation of the N(11), N(12), N(13), and O(11) atoms with regard to their mean basal plane is 0.12 Å; still, Cu(1) is displaced toward the apical site by 0.11 Å. The dihedral angles between the basal plane, formed by the N(11), N(12), N(13), and O(11) atoms and the carboxylate groups, as well as the one between the former plane and the benzene ring are 21.5 and 3.9°, respectively.

The Cu(2) center is in 4 + 2 surroundings. The basal plane includes the three N(21), N(22), and N(23) atoms of another dien ligand as well as the O(21) atom of the second carboxylate group of the Phth bridging unit. The two axial positions are occupied by the O(22) atom of the same carboxylate group of Phth and the symmetrically related O(22') atom of a neighboring phthalato ligand. Due to the unequal Cu(2)–O(22) = 2.800 (8) Å and Cu(2)–O(22') = 2.318 (8) Å bond distances (see Table III) and the O(21)–Cu(2)–O(22) = 52.0 (3)°, N(22)–Cu(2)–O(22) = 116.8 (3)°, and N(22)–Cu(2)–O(22') = 97.1 (3)° angles (Table IV) the local geometry around Cu(2) could be regarded as a severely distorted octahedral one. The largest deviation of the N(21), N(22), N(23), and O(21) atoms from their mean basal plane is 0.2 Å, whereas Cu(2) deviates only by 0.07 Å. Moreover, this basal plane is almost perpendicular to its neighboring carboxylate group plane (80.5°) and approximately parallel to the benzene ring's plane (dihedral angle 11.2°).

Table IV. Main Bond Angles (deg)[a]

Cu Surroundings			
Cu(2)–O(22)–Cu(2')	109.0 (3)	O(22')–Cu(2)–O(22)	145.8 (4)
N(11)–Cu(1)–N(12)	83.8 (4)	N(21)–Cu(2)–N(22)	84.6 (4)
N(11)–Cu(1)–N(13)	163.2 (5)	N(21)–Cu(2)–N(23)	166.5 (4)
N(12)–Cu(1)–N(13)	84.4 (4)	N(22)–Cu(2)–N(23)	84.4 (4)
N(11)–Cu(1)–O(11)	90.8 (4)	N(21)–Cu(2)–O(21)	100.5 (3)
N(12)–Cu(1)–O(11)	174.2 (4)	N(22)–Cu(2)–O(21)	168.0 (4)
N(12)–Cu(1)–O(8)	93.6 (6)	N(22)–Cu(2)–O(22)	116.8 (3)
O(21)–Cu(2)–O(22')	94.0 (3)	O(21)–Cu(2)–O(22)	52.0 (3)
		N(22)–Cu(2)–O(22')	97.1 (3)
Bridging Phthalato Ligand			
C(1)–O(11)–Cu(1)	126.3 (7)	C(2)–O(21)–Cu(2)	110.7 (7)
O(11)–C(1)–O(12)	126.7 (8)	O(21)–C(2)–O(22)	122.5 (9)
O(12)–C(1)–C(111)	119.1 (8)	O(21)–C(2)–C(116)	116.0 (9)
C(1)–C(111)–C(116)	121.4 (9)	C(2)–C(116)–C(111)	123.1 (7)
C(112)–C(111)–C(116)	118.0 (7)	C(115)–C(116)–C(111)	118.8 (9)
Diethylenetriamine Ligands			
Cu(1)–N(11)–C(13)	112.1 (9)	Cu(2)–N(21)–C(22)	109.6 (6)
N(11)–C(13)–C(14)	108.0 (1)	N(21)–C(22)–C(21)	108.4 (8)
C(13)–C(14)–N(12)	107.0 (1)	C(22)–C(21)–N(22)	106.0 (1)
C(14)–N(12)–C(12)	118.0 (1)	C(21)–N(22)–C(23)	117.4 (9)
C(14)–N(12)–Cu(1)	107.8 (7)	C(21)–N(22)–Cu(2)	108.9 (7)
Perchlorate Anions			
O(1)–C(11)–O(2)	110.5 (7)	O(5)–C(12)–O(8)	101.0 (1)
O(2)–C(11)–O(4)	113.0 (1)	O(6)–C(12)–O(8)	87.0 (1)

[a] Standard deviations of the last significant figures are given in parentheses.

All Cu–N bond distances, ranging from 1.99 (2) to 2.016 (7) Å, are comparable with the ones found in other Cu(II) amine complexes.[13,14] The Cu–O "short" distances of 1.927 (5) and 2.010 (7) Å are also in line with the corresponding ones found in μ-phthalato[15] and μ-terephthalato[4,16] complexes. The "long" Cu–O distances of 2.318 (8), 2.46 (2), and 2.800 (8) Å are also comparable with the corresponding ones found in the aforementioned Cu(II) complexes.

The distance between Cu(1) and Cu(2), connected by the same Phth ligand, is 6.704 (4) Å, and the shortest Cu(2)···Cu(2') one, along the same chain, is 4.180 (3) Å.

The six carbon atoms of the benzene ring of the Phth do not deviate more than 0.01 Å from their respective mean plane. The dihedral angles between the carboxylate planes and the benzene ring are 17.7° [C(1), O(11), O(12)] and 89.0° [C(2), O(21), O(22)]; the dihedral angle between the two carboxylate groups of Phth is 78.7°. The carboxylate C(1) atom is coplanar with the mean benzene plane, whereas C(2) deviates by 0.15 Å from it.

Finally, the noncoordinated perchlorate ion exhibited large thermal ellipsoids due to orientational disorder.

Spectroscopic Data of the Complex. In the IR region of the spectrum the complex exhibited the two characteristic strong and

(12) Johnson, C. K. ORTEP II. Report ORNL-5138; Oak Ridge National Laboratory: Oak Ridge, TN, 1976, Vol 22, p 833.

(13) (a) Brown, B. W.; Lingafelter, E. C. *Acta Crystallogr.* **1964**, *17*, 254. (b) Komiyama, Y.; Lingafelter, E. C. *Ibid.* **1964**, *17*, 1145.

(14) Morpurgo, G. O.; Mosini, V.; Porta, P. *J. Chem. Soc., Dalton Trans.* **1981**, *111*.

(15) Krstanovic, I.; Karanovic, Lj.; Stojakovic, Dj. *Acta Crystallogr.* **1985**, *C41*, 43 and references therein.

(16) Verdaguer, M.; Gouteron, J.; Jeannin, S.; Jeannin, Y.; Kahn, O. *Inorg. Chem.* **1984**, *23*, 4291.

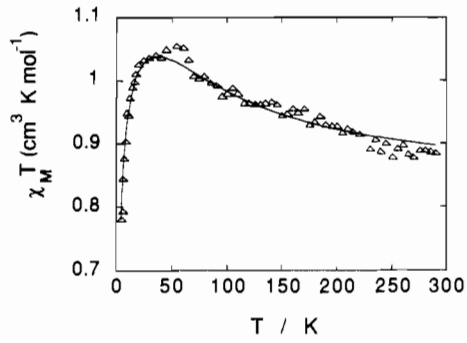

Figure 3. Experimental (triangles) and theoretical (solid line) temperature dependence (290–4.2 K) of $\chi_{Cu}T$.

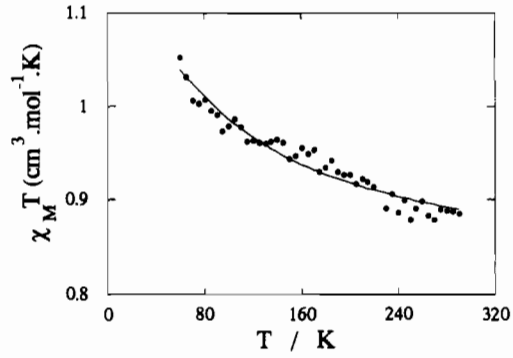

Figure 4. Experimental (circles) and theoretical (solid line) temperature dependence (290–60 K) of $\chi_{Cu}T$.

broad bands in the 1700–1300-cm^{-1} region, attributed to the $\nu_{as}(CO_2)$ (1578 cm^{-1}) and $\nu_s(CO_2)$ (1375 cm^{-1}) stretching vibrations of the coordinated carboxylato groups. These two bands were separated by ca. 203 cm^{-1}, suggesting[17] an anisobidentate coordination mode for both carboxylato groups of the $Phth^{2-}$ ligand. Moreover, the characteristic bands due to the $\nu(NH_2)$ stretchings of the dien ligand at ca. 3138, 3172, and 3255 cm^{-1}, as well as the ν(Cl–O) stretching–a strong broad weakly split band at ca. 1100 cm^{-1}, suggesting[18] a weak unidentate coordination for the ClO_4^- anion—were also seen.

The electronic reflectance spectrum of the compound—a broad-band envelope with a maximum at ca. 16 100 cm^{-1} and a shoulder at ca. 19 510 cm^{-1}—could be also in line with the coexistence[19] of a square-pyramidal and a distorted elongated octahedral and/or square-planar chromophore.

The room-temperature X-band EPR spectrum of the complex exhibited a single, slightly asymmetric signal (g = 2.083) as a result of overlapping signals of two Cu(II) ions in different environments.[20]

Magnetic Data and Their Interpretation. Variable-temperature (4.2-290 K) magnetic susceptibility data were collected for a solid sample of the complex.

The magnetic behavior of the complex, in the form of a $\chi_M T$ vs T plot, is depicted schematically in Figure 3. At 290 K the experimental $\chi_M T$, χ_M being the molar magnetic susceptibility for the binuclear unit, is equal to 0.885 cm^3 mol^{-1} K. When the sample is cooled down from room temperature, $\chi_M T$ increases in a smooth fashion and reaches a maximum at about 60 K with $\chi_M T$ = 1.052 cm^3 mol^{-1} K and then remains at a constant plateau down to 20 K. Below 20 K, $\chi_M T$ decreases rapidly to a value of 0.780 cm^3 mol^{-1} K at 4.2 K [full-length table of magnetic data—experimental and calculated χT values—are given as supplementary materials (Tables SVII and SVIII)].

The interpretation of the magnetic behavior in the 20–290 K temperature range is straightforward. The exchange interaction between the two single-ion spin doublets leads to two molecular levels characterized by S = 0 and S = 1, respectively, and separated by J. J is positive if the spin triplet is the lowest level. At room temperature the $\chi_M T$ value is slightly higher than that expected (ca. 0.80 cm^3 mol^{-1} K) for two noncoupled copper(II) ions. The increase of the $\chi_M T$ upon cooling down shows that the S = 1 level is actually the lowest in energy. Below 60 K, the S = 0 level is totally depopulated, with a $\chi_M T$ value (ca. 1.1 cm^3 mol^{-1} K) corresponding[21] to a ferromagnetically coupled copper(II) dimer. Finally, the decrease of the $\chi_M T$ values below ca. 20 K is most likely due to an interdimer antiferromagnetic coupling between the S = 1 molecular spins.

Considering the structure, two exchange pathways are possible: one through the carboxylato group bridging the two neighboring Cu(2) atoms along the same chain unit; the other one through the phthalato dianion bridging the Cu(1) and Cu(2) atoms of the same binuclear unit. Although the crystal structure suggests an one-dimensional chain structure, the magnetic data indicate that the compound rather behaves magnetically as a chain of weakly interacting binuclear units. Therefore, in a first approach, a least-squares fit of the experimental data from room temperature down to 4.2 K was attempted with a molecular field approximation[22] in order to account for the interdimer interactions of the complex. In the frame of this approximation (with the interaction Hamiltonian $\mathcal{H} = -J\hat{S}_1\hat{S}_2$) values of +80 cm^{-1}, 2.099, and −1.81 cm^{-1} were obtained for J, g, and zJ', respectively, with a very good R value of $R = 1.54 \times 10^{-4}$ [R is the agreement factor defined as $R = \sum_i[(\chi_{obsd})_i - (\chi_{theor})_i]^2/\sum_i(\chi_{obsd})_i^2$]. In a three-parameter fitting with J, g, and zJ' variables, a J value of +80 cm^{-1} was obtained along with a theoretical g value almost identical with the experimental one. The question that immediately arises is then does the calculated J value has a physical sense or it is just a mathematical result?

In an attempt to check this a second fitting was attempted in the high-temperature range in order to exclude the intermolecular interactions. As a matter of fact, the 290–60 K experimental data were interpreted with a simple Bleaney–Bowers equation.[23] The curve calculated under this assumption fits very well with the experimental points (see Figure 4), leading to almost the same J values as before (+83 cm^{-1}), along with a slightly better R value (1.24×10^{-4}) than the previous procedure. During this procedure, the g value was kept constant and equal to the EPR one of the complex, g = 2.083.

Consequently, it seems quite appropriate to employ in our case the molecular field approximation. Hence, a J value of 80 ± 10 cm^{-1} for the singlet–triplet splitting along with a J' value of −0.91 cm^{-1} (for z = 2) is proposed for the complex under investigation.

The question asked now is as follows: Is it possible to rationalize the inter- and intradimer interactions on an orbital basis? In an attempt to answer this question the experimental results discussed above are combined with the quantum-chemical results of the EHMO type in the next section.

Orbital Interpretation of the Exchange Mechanism. The ability of the carboxylate group to propagate the exchange interaction between two Cu(II) ions separated by more than 5 Å has well been demonstrated in the case of (μ-oxalato) copper(II) compounds.[24,25] As a matter of fact, due to the syn–syn configuration[26] of its carboxylato bridge (see **1**),[27] a $2J/k$ value of −558 K was found[24] in $[(tmen(H_2O)Cu(C_2O_4)Cu(H_2O)tmen](ClO_4)_2$ with a Cu–Cu separation of 5.14 Å. However, due to the anti–syn

(17) Deacon, G. B.; Phillips, R. J. *Coord. Chem. Rev.* **1980**, *33*, 227.
(18) Wickenden, A. E.; Krause, R. A. *Inorg. Chem.* **1965**, *4*, 404.
(19) Hathaway, B. J.; Tomlinson, A. G. *Coord. Chem. Rev.* **1970**, *5*, 1.
(20) Felthouse, T. R.; Laskowski, E. J.; Bieksza, D. S.; Hendrickson, D. N. *J. Chem. Soc., Chem. Commun.* **1976**, 777.
(21) Kahn, O.; Galy, J.; Journaux, Y.; Jaud, J.; Morgenstern-Badarau, I. *J. Am. Chem. Soc.* **1982**, *104*, 2165.
(22) Ginsberg, A. P.; Lines, M. E. *Inorg. Chem.* **1972**, *11*, 2289.
(23) Bleaney, B.; Bowers, K. D. *Proc. R. Soc. A* **1952**, *250*, 451.
(24) Julve, M.; Verdaguer, M.; Gleizes, A.; Philoche-Levisalle, M.; Kahn, O. *Inorg. Chem.* **1984**, *23*, 3808.
(25) Michalowicz, A.; Girerd, J. J.; Goulon, J. *Inorg. Chem.* **1979**, *11*, 3004.
(26) Pei, Y.; Nakatani, K.; Kahn, O.; Sletten, J.; Renard, J.-P. *Inorg. Chem.* **1986**, *16*, 3170.
(27) Carlin, L. R.; Kopinga, A.; Kahn, O.; Verdaguer, M. *Inorg. Chem.* **1986**, *25*, 1786.

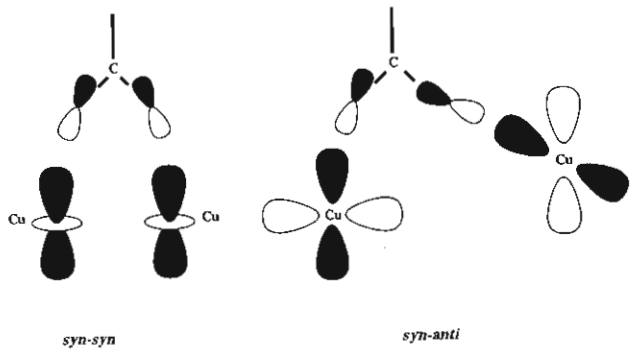

1

configuration of its carboxylato bridge, the $[Cu(NH_3)_2(CH_3CO-O)Br]$ polymeric complex exhibited[27] a J/k value of −4.3 K. The problem at hand is then this: How strong would the exchange through the O(21)–C(2)–O(22) carboxylate bridge be?

On the basis of the results of EHMO calculations, carried out with the crystal data available for our complex, the unpaired electron around each Cu(2) magnetic center is mainly described by a magnetic orbital of $x^2 - y^2$-type (see **2**) pointing toward the

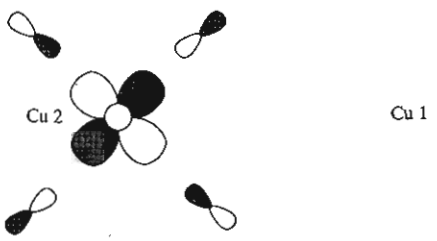

2

four nearest neighbors—O(21), N(21), N(22), and N(23) atoms—in the equatorial plane. That, along with the rather large Cu(2)–O(22′) distance, rules out a strong interaction through the O(22′) atom, which is perpendicular to the plane of the magnetic orbital. However, due to some admixture of a z^2-type orbital pointing toward the O(22′) atom in the apical position, a weak interdimer interaction through this latter atom should not be excluded. Moreover, along the chain structure, the magnitude of the antiferromagnetic interaction is governed by the overlap of two magnetic orbitals of this kind centered on the nearest-neighbor Cu(2) ions.[28] Owing to the symmetry of the Cu(2)–O(21)–C(2)–O(22)–Cu(2′) bridging network, with a syn–anti carboxylato-bridge configuration (see **3**), the contributions of the

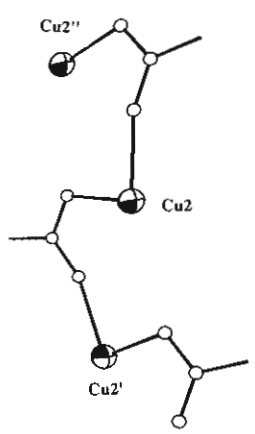

3

2p orbitals of O(21) and O(22), belonging to the magnetic orbitals centered on Cu(2) and Cu(2″), respectively, are unfavorably

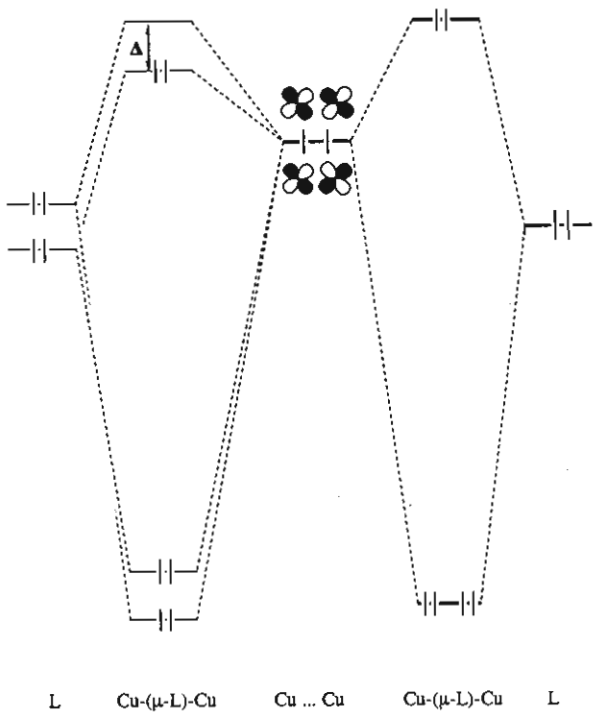

Figure 5. Molecular orbital diagram, showing the interactions between the two in- and out-of-phase d-orbital combinations of the two Cu(II) ions with the symmetry-adapted ligand orbitals leading to the two degenerate (right-hand side) and to the two nondegenerate (top left-hand side) MO's of the dimer.

oriented to give a strong overlap.

The intradimer interaction is examined next. Hoffmann et al.[29] have developed an orbital model for the superexchange interactions. On the basis of this approach, the singlet–triplet splitting $E_S - E_T$, for the interaction of two $^1/_2$ ions can be expressed by the combination of a ferromagnetic term, denoted as J_F, and an antiferromagnetic one, J_{AF}:

$$E_T - E_S = 2J = J_F + J_{AF} = -2K_{ab} + (\epsilon_1 - \epsilon_2)^2/(J_{aa} - J_{ab})$$

Here all symbols have their usual meaning. For the degenerate case $\epsilon_1 = \epsilon_2$, the triplet state is the ground state:

$$E_S - E_T = 2K_{ab} \qquad K_{ab} > 0$$

Moreover, J_{AF} is related to the square of the energy separation Δ ($=\epsilon_1 - \epsilon_2$) between the two highest occupied SOMO's. The larger Δ^2, the stronger the antiferromagnetic interaction. Since Δ^2 can be easily derived by means of semiempirical MO calculations, as a function of various molecular parameters, it is possible to predict qualitatively the effect that changes in molecular geometry will have on the strength of the exchange coupling. The usual situation encountered is shown on the left-hand side of Figure 5. The in- and out-of-phase d-orbital combinations are degenerate, owing to the absence of direct d–d interactions. However, the symmetry-adapted ligand orbitals are not degenerate. This leads to an energy gap Δ between the two SOMO's of the binuclear complexes, thus leading predominantly to antiferromagnetic exchange interactions.

The results of the EHMO calculations, performed on the phthalato dianion, have shown that δ, being the energy difference between the symmetric and antisymmetric MO's of the bridging ligand, symmetry-adapted to interact with the degenerate single-occupied in- and out-of-phase combinations of the d_{xy} metal orbitals [the x axis being defined by Cu(1)···Cu(2)], is decreased as ω, being the angle between the planes of the two carboxylato groups of the phthalato dianion, increases (see Figure 6). As a matter of fact, the energy-difference minimum corresponds to

(28) Girerd, J. J.; Charlot, M. F.; Kahn, O. *Mol. Phys.* **1977**, *34*, 1063.

(29) Hay, P. J.; Thibeault, J. C.; Hoffmann, R. J. *J. Am. Chem. Soc.* **1975**, *97*, 4884.

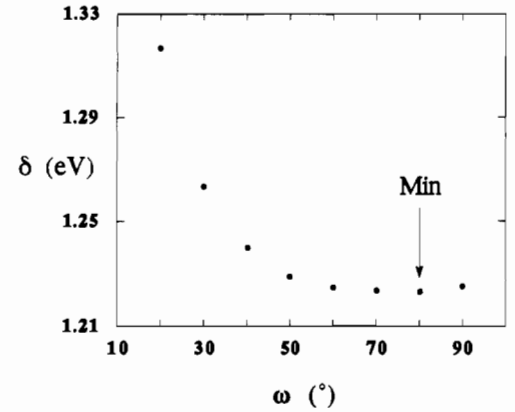

Figure 6. Variation of the energy difference between the symmetric and antisymmetric MO's of the bridging ligand, δ, with the angle between the planes of the carboxylato groups of the phthalato dianion, ω.

an ω value of ca. 80°, this latter value being the crystallographic angle between the two carboxylato groups of the phthalato bridge. These results clearly show that the variations in ω should play a significant role on the antiferromagnetic coupling of the complex and/or an ω value of ca. 80° should minimize the antiferromagnetic contribution in the exchange coupling.

Consequently, EHMO calculations could provide a reasonable orbital basis for a qualitative understanding of the relative merit of the ω angle in determining the strength of the magnetic exchange interactions in the phthalato-bridged copper(II) dimers. Moreover, although it is too early for general conclusions to be drawn, it seems probable that a new situation stems leading to ferromagnetic exchange interactions through extended bridging ligands, which is based mainly on the topology of the intervening bridge. More work along this line is under way in our laboratory.

Acknowledgment. We acknowledge Dr. Alain Michalowitcz and Dr. Daniel Andre (Laboratoire de Physico-Chimie Structural, Université Paris Val de Marne, 94000 Creteil, France) for making their Macintosh Ortep[12] version available to us and for their help in using the program. Mac Ortep is available on request, from A.M. and/or D.A.

Supplementary Material Available: Tables SI-SV and SVII, listing a summary of the crystallographic data collection, anisotropic temperature coefficients U_{ij} for the non-hydrogen atoms, atomic parameters for the hydrogen atoms, interatomic distances, bond angles, and experimental and calculated magnetic susceptibility data (9 pages); Table SVI, listing calculated and observed structure factors (20 pages). Ordering information is given on any current masthead page.

Contribution from the Chemical Crystallography Laboratory, University of Oxford, Oxford OX1 3PD, U.K., Department of Chemistry, Northeastern University, Boston, Massachusetts 02115, and Experimental Station, Central Research and Development,[1] E. I. du Pont de Nemours and Company, Wilmington, Delaware 19880-0356

A New Ferric Orthoarsenate Hydrate: Structure and Magnetic Ordering of $FeAsO_4 \cdot {}^3/_4H_2O$

R. J. B. Jakeman,[2a] M. J. Kwiecien,[2b,c] W. M. Reiff,*[,2b] A. K. Cheetham,*[,2a] and C. C. Torardi*[,2d]

Received July 3, 1990

A new hydrated form of $FeAsO_4$ has been synthesized and its crystal structure determined. $FeAsO_4 \cdot {}^3/_4H_2O$ crystallizes in a triclinic cell, $P\bar{1}$, with cell constants a = 6.600 (2) Å, b = 9.015 (2) Å, c = 6.539 (1) Å, α = 104.39 (2)°, β = 104.40 (2)°, γ = 84.25 (2)°, V = 364.7 Å^3, and Z = 4. It exhibits a novel tetrameric unit of iron octahedra, two FeO_6 and two $FeO_5(H_2O)$, that share edges. These units are interconnected by AsO_4 tetrahedra to create a network structure having open channels containing the water molecules bonded to iron as well as water of hydration. Mössbauer spectroscopy measurements over the range T = 298-4.2 K reveal a transition to a three-dimensional magnetically ordered state at ~47.5 K. The Zeeman-split spectra allow for resolution of the two inequivalent iron sites for which internal hyperfine fields of H_n = 535 and 526 kG have been determined at 4.2 K. Magnetic susceptibility measurements indicate antiferromagnetic order below ~49 K in agreement with the Mössbauer spectroscopy results, with the paramagnetic Curie temperature $\Theta \sim -128$ K. The magnetic moment calculated from the Curie-Weiss fit in the paramagnetic region is 5.68 μ_B. The magnitude of $T_{Néel}$ for $FeAsO_4 \cdot {}^3/_4H_2O$ (=$Fe_4(AsO_4)_4 \cdot 3H_2O$) is compared to $T_{Néel}$ for other antiferromagnetically ordered iron(III) arsenate compounds.

Introduction

For several years, we have studied the structures and related magnetic properties of transition-metal compounds containing bridging tetrahedral oxyanions such as PO_4^{3-}, AsO_4^{3-}, SO_4^{2-}, and MoO_4^{2-}. Of these, the compounds of iron have been of special interest and include $Fe_4(OH)_3(PO_4)_3$,[3] layered $FeClMoO_4$ and its alkali-metal insertion compounds,[4] open-framework $Fe_2(SO_4)_3$,[5] and $Fe_2(MoO_4)_3$[6] and its Li insertion compound $Li_2Fe_2(MoO_4)_3$.[7] Such materials are of interest because of their potential as catalysts or as battery materials in electrochemical devices. Prior to our structural determination of anhydrous $FeAsO_4$ by neutron powder diffraction,[8] we tried to grow crystals of this phase by hydrothermal methods. Instead, we isolated a new hydrated form of ferric arsenate having an interesting tunnel arrangement of atoms, which will be discussed in this paper.

The naturally occurring mineral scorodite, $FeAsO_4 \cdot 2H_2O$, is a related hydrated ferric arsenate compound for which Mössbauer spectroscopy,[9,10] magnetic susceptibility,[10] and X-ray crystallog-

(1) Contribution No. 5534.
(2) (a) University of Oxford. (b) Northeastern University. (c) Current address: Gillette Corp., Boston, MA. (d) E. I. du Pont de Nemours and Co.
(3) Torardi, C. C.; Reiff, W. M.; Takacs, L. *J. Solid State Chem.* **1989**, *82*, 203.
(4) Torardi, C. C.; Reiff, W. M.; Lázár, K.; Prince, E. *J. Phys. Chem. Solids* **1986**, *47*, 741.
(5) Takacs, J.; Takacs, L.; Reiff, W. M.; Torardi, C. C. *Hyperfine Interact.* **1988**, *40*, 347.
(6) Battle, P. D.; Cheetham, A. K.; Long, G. J.; Longworth, G. *Inorg. Chem.* **1982**, *21*, 4223.
(7) Reiff, W. M.; Zhang, J. H.; Torardi, C. C. *J. Solid State Chem.* **1986**, *62*, 231.
(8) Cheetham, A. K.; David, W. I. F.; Eddy, M. M.; Jakeman, R. J. B.; Johnson, M. W.; Torardi, C. C. *Nature* **1986**, *320*, 46.
(9) Kiriyama, R.; Sakurai, K. *X-rays* **1949**, *5*, 85; *Struct. Rep.* **1949**, *12*, 251.

0020-1669/91/1330-2806$02.50/0